Three-dimensional analysis of magnetotelluric data from the New Afton porphyry deposit, central British Columbia

E. Roots[1, 2*], J.A. Craven[2], E. Schetselaar[2], R. Enkin[3], and D. Wade[4]

Roots, E., Craven, J.A., Schetselaar, E., Enkin, R., and Wade, D., 2021. Three-dimensional analysis of magnetotelluric data from the New Afton porphyry deposit, central British Columbia; in *Targeted Geoscience Initiative 5: contributions to the understanding and exploration of porphyry deposits, (ed.) A. Plouffe and E. Schetselaar; Geological Survey of Canada, Bulletin 616, p. 53–64. https://doi.org/10.4095/327952*

Abstract: Magnetotelluric data were collected along eight lines perpendicular to the mineralized zone and alteration halo of the New Afton Cu-Au porphyry deposit. The data were collected at an interstation spacing of 100 m and a line spacing of 300 m, and with a bandwidth of approximately 0.01 to 10 000 Hz. Phase tensor maps show an approximately east-west delineation of the survey into northern and southern sections. Determinant phase maps show conductivities initially increasing with depth in the north and decreasing in the south, with this trend reversing at depth. Preliminary results from 3-D inversions show conductive cover underlain by more resistive material throughout most of the survey area, with notably lower resistivities to the north. Two linear northeast-southwest features, spatially associated with the New Afton and Pothook mineralization, are imaged crosscutting the primary east-west fault zone, with high resistivities in the north and low resistivities in the south.

Résumé : Des données magnétotelluriques ont été recueillies le long de huit lignes perpendiculaires à la zone minéralisée et à l'auréole d'altération du gisement porphyrique à Cu-Au de New Afton. Les données ont été recueillies suivant un espacement entre les stations de 100 m et un espacement entre les lignes de 300 m, dans une largeur de bande d'environ 0,01 à 10 000 Hz. Les cartes des tenseurs de phase montrent une limite grossièrement est-ouest séparant l'aire du levé en une section nord et une section sud. Les cartes des phases du déterminant montrent d'abord une augmentation de la conductivité en fonction de la profondeur dans le nord, et une diminution dans le sud, avec une inversion de cette tendance en profondeur. Les résultats préliminaires des inversions 3D montrent une couche conductrice reposant sur des matériaux plus résistifs dans la plus grande partie de l'aire du levé, et des résistivités significativement plus faibles au nord. Des données d'imagerie montrent que deux entités linéaires d'orientation nord-est–sud-ouest, associées sur le plan spatial aux minéralisations de New Afton et de Pothook, recoupent la zone de failles principale est-ouest, avec de fortes résistivités au nord et de faibles résistivités au sud.

[1]Mineral Exploration Research Centre, Laurentian University, 935 Ramsey Lake Road, Sudbury, Ontario P3E 2C6
[2]Geological Survey of Canada, 601 Booth Street, Ottawa, Ontario K1A 0E8
[3]Geological Survey of Canada, 9860 West Saanich Road, Sidney, British Columbia V8L 4B2
[4]New Gold Inc., 4050 West Trans Canada Highway, Kamloops, British Columbia V1S 2A3
*Corresponding author: E. Roots (email: eroots@laurentian.ca)

INTRODUCTION

Electromagnetic methods have been widely used for mineral exploration due to their sensitivity and ability to resolve features associated with mineralization. As shallow targets have become increasingly scarce, the ability to image targets at depth as well as the deeper structures controlling mineralization has become increasingly important. The magnetotelluric (MT) method is an electromagnetic technique that can image at great depths compared to many controlled-source prospecting methods. As such, the use of the MT method as an exploration tool is becoming more popular in exploration for uranium (e.g. Heinson et al., 2006, 2018; Farquharson and Craven, 2009), diamonds (e.g. Jones et al., 2009; Türkoğlu et al., 2009), and base and precious metals (e.g. Zhang et al., 1995; Stevens and McNeice, 1998). The use of the MT method was previously restricted to 1-D and 2-D cases, limiting its applicability in complex geological environments; however, 3-D inversion of MT data is now becoming routine due to developments in inversion techniques and computational capabilities during the past few decades (Siripunvaraporn et al., 2005; Egbert and Kelbert, 2012; Miensopust et al., 2013; Newman, 2014).

Presented here are preliminary results of the 3-D inversion of MT data collected at the New Afton porphyry deposit in British Columbia, Canada, as part of the Geological Survey of Canada's Targeted Geoscience Initiative 5. The New Afton deposit is an alkaline Cu-Au porphyry deposit, with mineralization consisting primarily of disseminated sulfides. Because disseminated sulfides are generally resistive due to the lack of interconnectivity between grains, the resistivity contrast between sulfides and their host rock is unlikely to be detectable using the MT data. Because of this, as with previous studies in this area (e.g. Bellefleur et al., 2019), the focus of our investigation is on imaging alteration envelopes and structures controlling the emplacement of mineralization.

GEOLOGICAL SETTING

The New Afton Cu-Au porphyry deposit is hosted by Late Triassic Nicola Formation fragmental and crystalline volcanic rocks (referred to as the BXF hereafter) and, to a lesser extent, by the 204 Ma Cherry Creek monzonite of the Iron Mask batholith (J. Lipske and D. Wade, unpub. rept., 2014; Bergen et al., 2015). The Nicola Formation is unconformably overlain by clastic sedimentary and volcanic rocks of the Eocene Kamloops Group.

The primary hypogene ore zone of the New Afton deposit (Fig. 1) consists of disseminated chalcopyrite and bornite and has a subvertical southwest plunge that is largely coincident with potassic alteration. The hypogene ore zone is structurally controlled by two subvertical southwest-northeast-striking fault zones, known as the Footwall and Hanging Wall faults. The BXF is juxtaposed by the Hanging Wall fault against a subvertical body of a serpentinized picrite unit, whose margin is characterized by a high-strain zone of brittle-ductile deformation. Numerous moderately to steeply dipping fault zones controlling late hypogene mineralization cut the primary ore. Supergene mineralization, consisting of native copper and chalcocite within hematite-rich oxidation zones, is more abundant at higher structural levels near the open pit, but native copper also extends to 700 m below the surface, beneath the pit and along older, long-lived structures.

The Pothook Cu-Au mineralization, located 1 km southeast of the New Afton deposit (Fig. 1) is characterized by a network of supergene and chalcopyrite-bornite-bearing veins hosted in dominantly Pothook diorite and lesser Nicola Formation volcanic rocks adjacent to younger, causative intrusions (Stanley, 1994). The centre of the historical pit, seen in drill core, contained a large body of hydrothermal breccia consisting of Pothook diorite, Nicola BXF, Cherry Creek monzonite, and Sugarloaf diorite that graded outward from a rotational to crackle breccia. Distribution of mineralization coincides with both potassic alteration associated with Cherry Creek monzonite and with albite alteration associated with the emplacement of the younger Sugarloaf diorite. Dykes, alteration, and mineralization are structurally controlled. The west side of the orebody is bounded by a sharp northwest-southeast contact represented by the locally faulted rheological picrite–Pothook diorite–BXF contact. Within the deposit and surrounding host rocks, the causative Cherry Creek monzonite and Sugarloaf diorite dykes also have a dominant northwest-southeast strike. Mapped supergene and chalcopyrite-bornite-bearing veins tend to be less regular, however, and have a dominant east-west-striking trend (Stanley, 1994).

DRILL CORE RESISTIVITY AND POROSITY MEASUREMENTS

Physical properties were measured in the GSC Pacific Paleomagnetism and Petrophysical Laboratory, following the methods outlined in GSC Open File 7227 (Enkin et al., 2012). Cylindrical subsamples, 2.5 cm in diameter and 2.2 cm long, were taken from 254 approximately 10 cm long pieces of split diamond-drill core selected to span the rock types and alterations present in the New Afton deposit. Porosity was measured by combining measurements of the dry, water-saturated, and water-immersed weights. Electrical resistivities are dependent on the resistivity of the pore water in the samples, which is approximated by allowing deionized water to dissolve pore-space solutes for 24 hours prior to measurement. The water was introduced under vacuum, and the beakers were shaken for 2 minutes, still under vacuum, to help the water infiltrate fine permeability pathways within the samples. The samples were placed between copper–copper sulfate electrodes, and the complex electric impedance

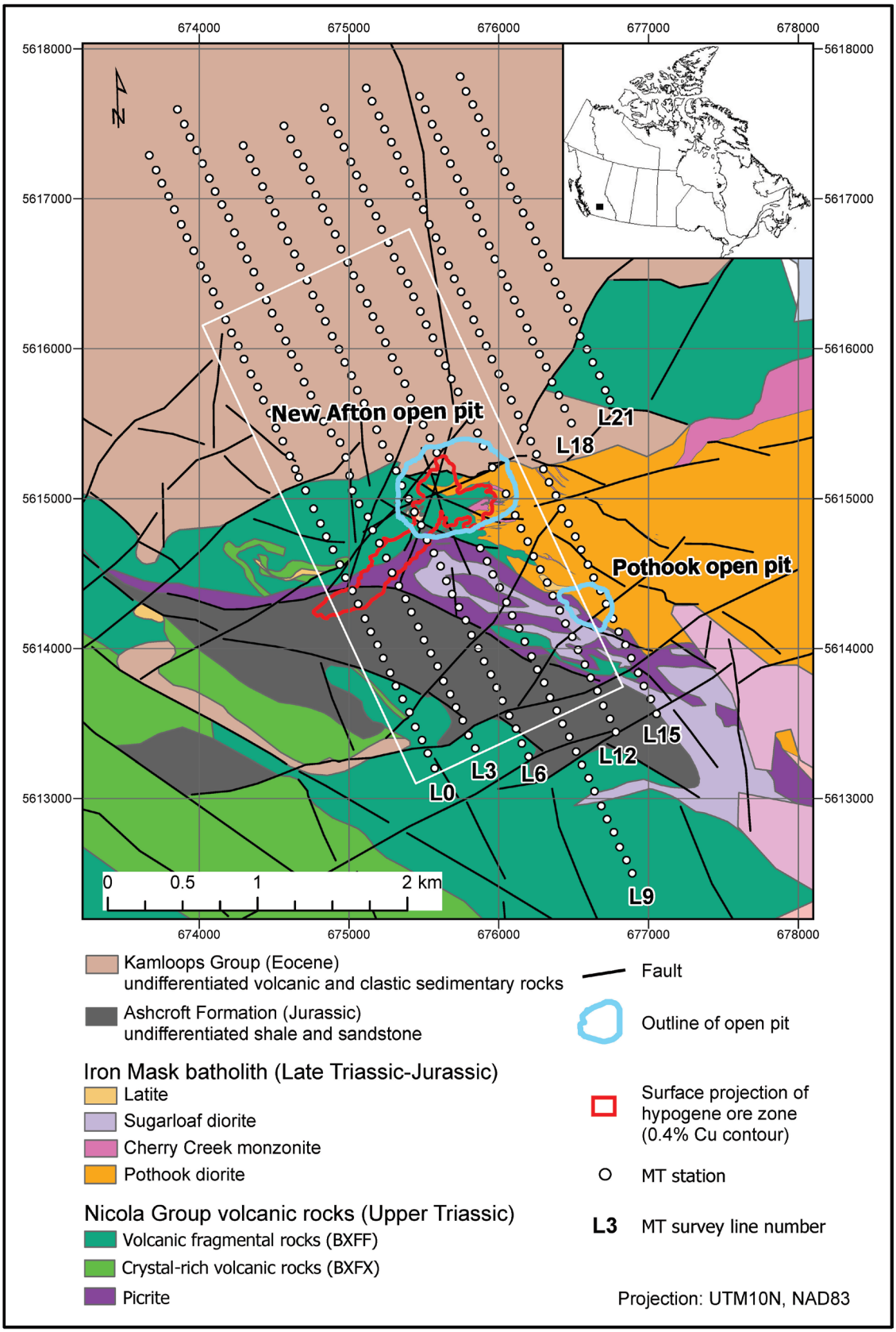

Figure 1. Map showing magnetotelluric (MT) stations and geology of the New Afton deposit. The white line indicates the subset of stations used in the presented focused inversion.

spectrum was measured using a Solartron 1260 impedance/gain-phase analyzer, at five frequencies per decade from 1 MHz down to 0.025 Hz. The resistivity at 0.1 Hz was measured after curve fitting and removing the very low frequency sample holder impedance. The resistivity is nearly inversely proportional to the porosity (Fig. 2). Excluding outliers, the best-fitting exponent is –1.2, with the implication that porosity is the major control on the resistivity in this data set.

MAGNETOTELLURIC DATA SET

Fieldwork was performed by Quantec Geoscience Ltd. in 2008 and 2009, with 332 audio-magnetotelluric (AMT) stations sampled (E. Gowan, T. Eadie, and R. Sharpe, unpub. rept., 2008). The stations were distributed across eight northwest-southeast-oriented lines, with a nominal interline spacing of 300 m and interstation spacing of 100 m (Fig. 1). Horizontal electric and magnetic fields were recorded and processed, resulting in MT impedance tensor measurements at frequencies between approximately 0.01 and 10 000 Hz. The data are generally of good quality between approximately 0.1 and 10 000 Hz with some degradation at lower frequencies. Mine infrastructure had an effect on the data quality in some locations; stations under major power lines or pipelines and near the highway have considerably higher errors at frequencies above 10 Hz, and those in areas with variable topography have slightly higher errors at frequencies below 0.5 Hz (E. Gowan, T. Eadie, and R. Sharpe, unpub. rept., 2008).

Analysis of the MT data was carried out using the phase tensor method (Caldwell et al., 2004). The phase tensor, Φ, is a 2 × 2 tensor that can be derived at each period of the MT impedance tensor and has the property of being independent of local site-dependent distortions created by small-scale (i.e. beneath the resolving power of the MT method) variations in near-surface geology. The phase tensor and its derived parameters can be visualized as ellipses (e.g. Fig. 3), which can be used to determine undistorted first-order characteristics of the MT data and therefore the geo-electric structure of the survey area. In 1-D environments, Φ is diagonal with equal components, and the corresponding ellipse reduces to a circle. In 2-D, Φ is symmetric, and can be made diagonal by multiplying it with a rotation matrix, where angle α represents the geo-electric strike direction with a 90° ambiguity. In the 3-D case, Φ is rotated again by a skew

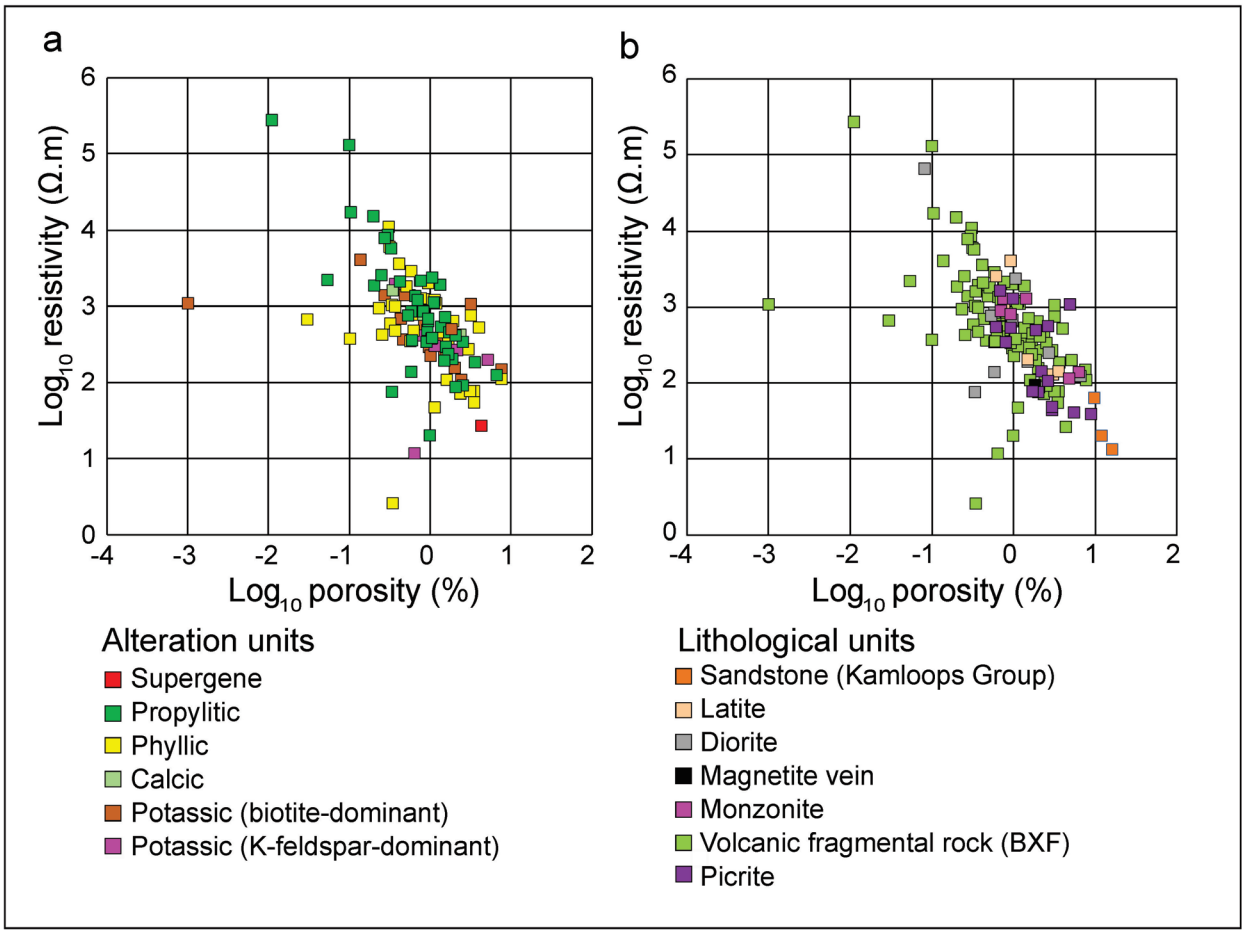

Figure 2. Resistivity-porosity scatterplots (log-scale) grouped according to **a)** lithological units and **b)** alteration units.

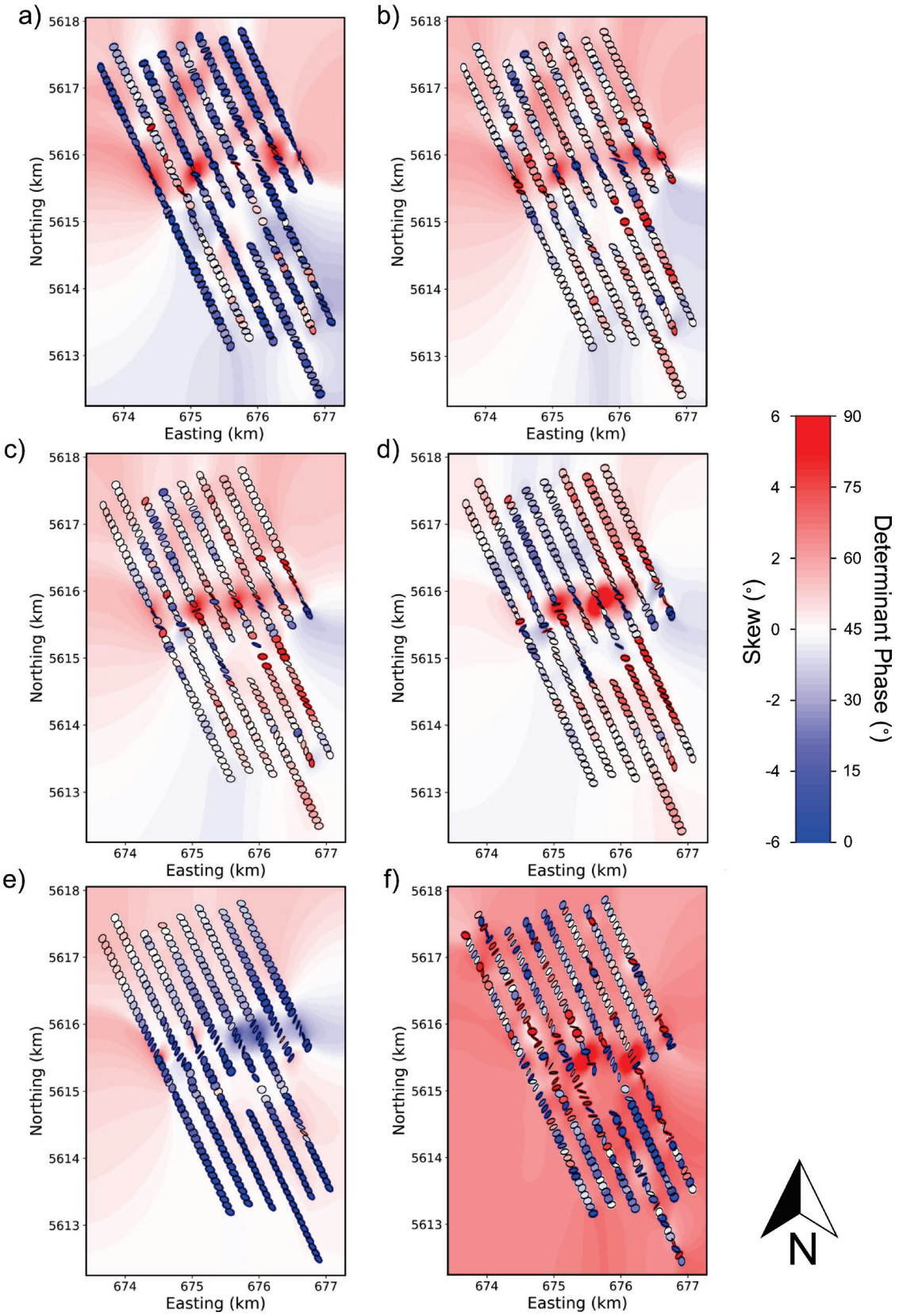

Figure 3. Plan view phase tensor maps of the magnetotelluric (MT) stations at various frequencies: **a)** 1500 Hz, **b)** 469 Hz, **c)** 143 Hz, **d)** 49.2 Hz, **e)** 2.46 Hz, and **f)** 0.111 Hz; background is coloured according to determinant phase; phase tensor ellipses are coloured by skew angle.

angle, β, representing a rotation of the phase tensor from an equivalent symmetric (i.e. 2-D) tensor. As such, analysis of the skew and azimuth values across a survey can be used to justify a 2-D or 3-D approach. Generally, for a 2-D approach to be valid, the strike directions must be consistent as a function of both space and frequency, and the skew values should be low (|β|<3; Caldwell et al., 2004; Booker, 2014). Furthermore, the determinant of the phase tensor, det|Φ|, with increasing period provides an estimate of increasing (det|Φ| increasing) or decreasing (det|Φ| decreasing) conductivity with increasing depth.

Determinant phase and skew angles across the survey area are shown in Figure 3. Between 1400 and 142.9 Hz, the area is separated into northern and southern sections by a sharp transition in phase, with generally high values (>60°) in the north and lower values (<45°) to the south. The relatively high phase in the north is consistent with the Kamloops sediments, which are generally porous and variably water saturated. At 49.2 Hz, the phase in the north drops to below 45°, possibly representing the base of the Kamloops Formation. At shorter frequencies (or equivalently, at greater depths), phases increase across most of the survey area to >45°, and exceed 70° at frequencies lower than 1 Hz, suggesting an underlying unit with relatively high conductivity. The phase tensor skew values are also frequency dependent, with generally low values (|β|<3) at frequencies between approximately 10 and 1000 Hz, and higher values outside of this range. Despite the relatively low skew values, the orientation of the phase tensor ellipses is highly variable. From north to south, the ellipses rotate clockwise until reaching a northing of approximately 5615 km, and then rotate back counterclockwise. A similar clockwise rotation goes from west to east, for example, at 2.4 Hz. These inconsistent azimuths combined with high skew values at the shorter frequencies suggest significant 3-D structure, necessitating the use of 3-D inversion for this data set.

THREE-DIMENSIONAL INVERSION

The 3-D inversion software ModEM (Kelbert et al., 2014) was used to produce 3-D resistivity models of the survey area. ModEM uses the standard Occam approach (Constable et al., 1987; de Groot-Hedlin and Constable, 1990), inverting the data to produce a model that minimizes the RMS misfit between the data and model response, as well as the gradient of the model conductivity. This produces spatially smooth models. Due to the large computational requirements of 3-D inversions, not all data could be inverted simultaneously; therefore, models were calculated at two scales: a regional scale that included every third station from all eight lines, and a focused scale using every station from a select area surrounding the ore zone (inside the solid white line in Fig. 1).

More than thirty inversions were performed to ensure the robustness of the produced models to changes in input parameters (e.g. mesh, rotation angle, starting model, inverted data points). In general, models at both scales agree where they overlap. Furthermore, the additional anomalies seen in the regional models tend to lie at the outer edge of the survey area and are not well constrained, so a preferred focused-scale model is presented in this paper. This inversion used a starting model with a half-space resistivity of 100 Ω-m and a mesh with 200 × 89 × 57 cells in the east-west, north-south, and vertical directions, respectively. A 165 × 50 cell inner mesh (Fig. 4) with 30 × 40 m cells was used directly around the stations, with exterior padding cell sizes increasing by a factor of 1.2. Although a uniform mesh is desirable, slightly elongated cells were required to stay within the limits of the available computational resources. To further optimize the mesh, the data were rotated by –25°, and a 25° rotation was applied to the station locations (or equivalently, a –25° rotation of the mesh) to ensure the inversion and measurement axes were aligned. The full impedance tensor was inverted using 19 logarithmically spaced frequencies between approximately 0.1 and 2400 Hz. Error floors were set to 5 and 10% for the off-diagonal and diagonal impedance components, respectively, with increased errors assigned to outliers. The inversion converged to an overall RMS of 1.7. Most stations have misfits of 1 to 2, but stations near the power lines north of the open pit have significantly reduced data quality and, therefore, have higher misfits of 3 to 6 (Fig. 4).

Plan view slices through the model are shown in Figure 5. Given the lateral cell sizes used, it is likely that the resistivity distributions at depths between 0 and 200 m are largely noise introduced by the inversions to accommodate static shifts and other local site distortion in the data. The trends seen in the phase tensor maps (Fig. 3) become evident in the model at depths of approximately 205 m, with the northern end of the survey having resistivities between approximately 1 and 30 Ω-m, whereas those in the south are between 100 and 1000 Ω-m with the exception of a few isolated regions, largely within the southeast corner. A linear resistive feature (R1) is seen between depths of 205 and 562 m with resistivities of approximately 300 to 500 Ω-m, trending parallel to southwest-northeast-trending secondary faults within the BXF unit. Toward the southeast, a smaller conductive zone (C1) runs parallel to the resistor. This conductor is partly associated with hypogene ore and the supergene alteration zone of the New Afton deposit. The larger R1 resistor cuts across most of the inverted stations, terminating just before the easternmost line (L12). At depth, R1 spreads into a broader region of high resistivity, at least partially as a result of the reduced resolving power of the MT method at depth. Approximately 2 km to the southeast, a second linear resistor-conductor pair (R2/C2) can be seen on the 316 and 562 m depth slices (Fig. 5b, c). The C2 conductor is also spatially associated with porphyry mineralization known as the Pothook deposit (Stanley, 1994), suggesting that economic mineralization in the surveyed area is structurally controlled in a consistent orientation. Another feature,

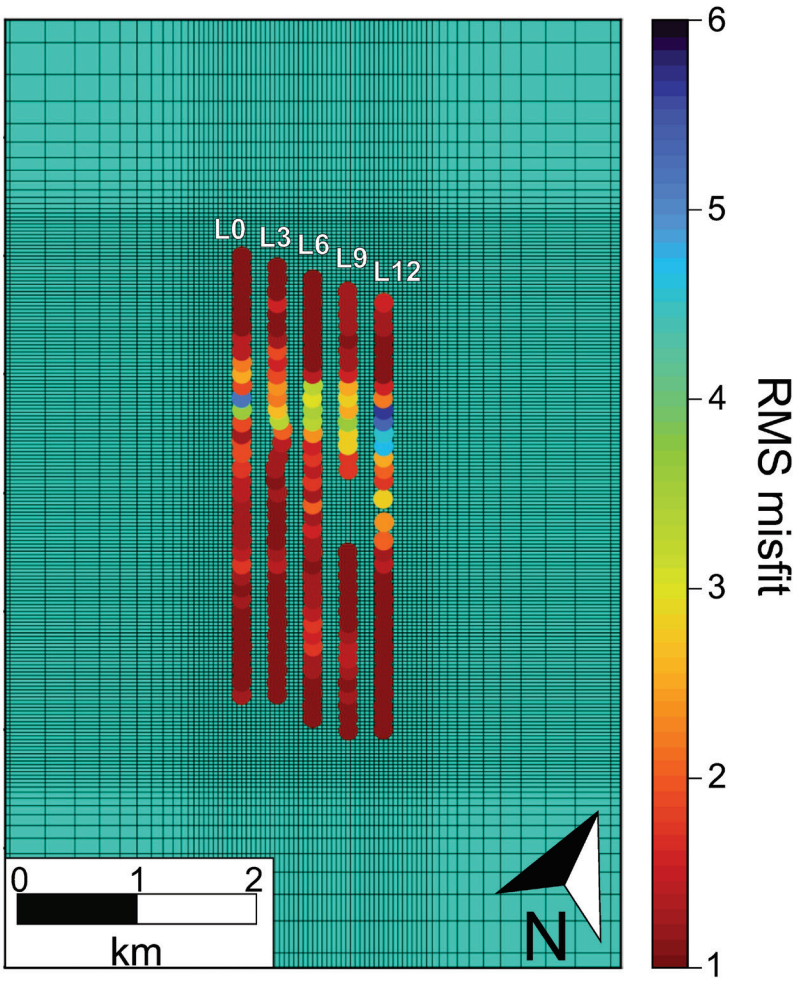

Figure 4. Interior mesh used in inversion and station layout (circles). Stations are coloured according to their respective RMS misfits from the preferred focused model.

C3, with resistivities between 1 and 10 Ω-m and oriented approximately east-west, is seen at similar depths and just to the north of R1. As with R1, C3 becomes more diffuse at depths below 500 m.

The geometry and extent of R1/C1 can be seen in depth slices through the model (Fig. 6), with R1/C1 moving progressively further north in each slice. It seems that R1 has a greater depth extent in comparison to C1, whereas C2 seems to have a greater depth extent in comparison to its resistive counterpart, R2 (Fig. 6). A west-southwest-east-northeast-striking conductor, C3, is visible to depths of approximately 500 m in the slices corresponding to L6, L9, and L12. The shallow depth and discordant strike direction suggest that C3 is associated with volcanic and sedimentary rocks of the Eocene Kamloops Group, unconformably overlying the volcanic rocks (mainly volcanic fragmentals of the Nicola Group) that host the porphyry deposits. Stratigraphically equivalent volcanic and sedimentary rocks elsewhere in Quesnellia have a similar conductive response (Spratt and Craven, 2011). A perspective view of the 3-D MT inversion model shows that the hypogene ore zone of the New Afton deposit is not associated with a conductive feature (Fig. 7).

DISCUSSION

The spatial association between the resistor-conductor pairs (C1/R1 and C2/R2) and their consistent southwest-northeast strike, parallel to fault zones established by drilling, strongly suggests that the mineralization is structurally controlled. Nevertheless, the geological significance of these features remains ambiguous, even for C1/R1, where information on the lithology, alteration, and ore mineral assemblages are available from the dense drillhole distribution of the New Afton mine workings. The discordant orientation in strike of C1/R1 and C2/R2 with respect to the dominant east-west strike of the lithological units and the lack of distinct lithology and alteration clusters in the log resistivity–porosity scatterplots (Fig. 2) indicate that variations in host rock mineralogical composition and associated primary porosity are most likely not the dominant factors controlling the resistivity contrasts between these features. Also, the hypogene ore zone with disseminated sulfide mineralization cannot explain C1 because only the extreme northern part of the ore zone coincides with the conductive zone. The largest part of the hypogene ore zone, toward the south, actually corresponds to resistor R1 (Fig. 7) and appears to be more

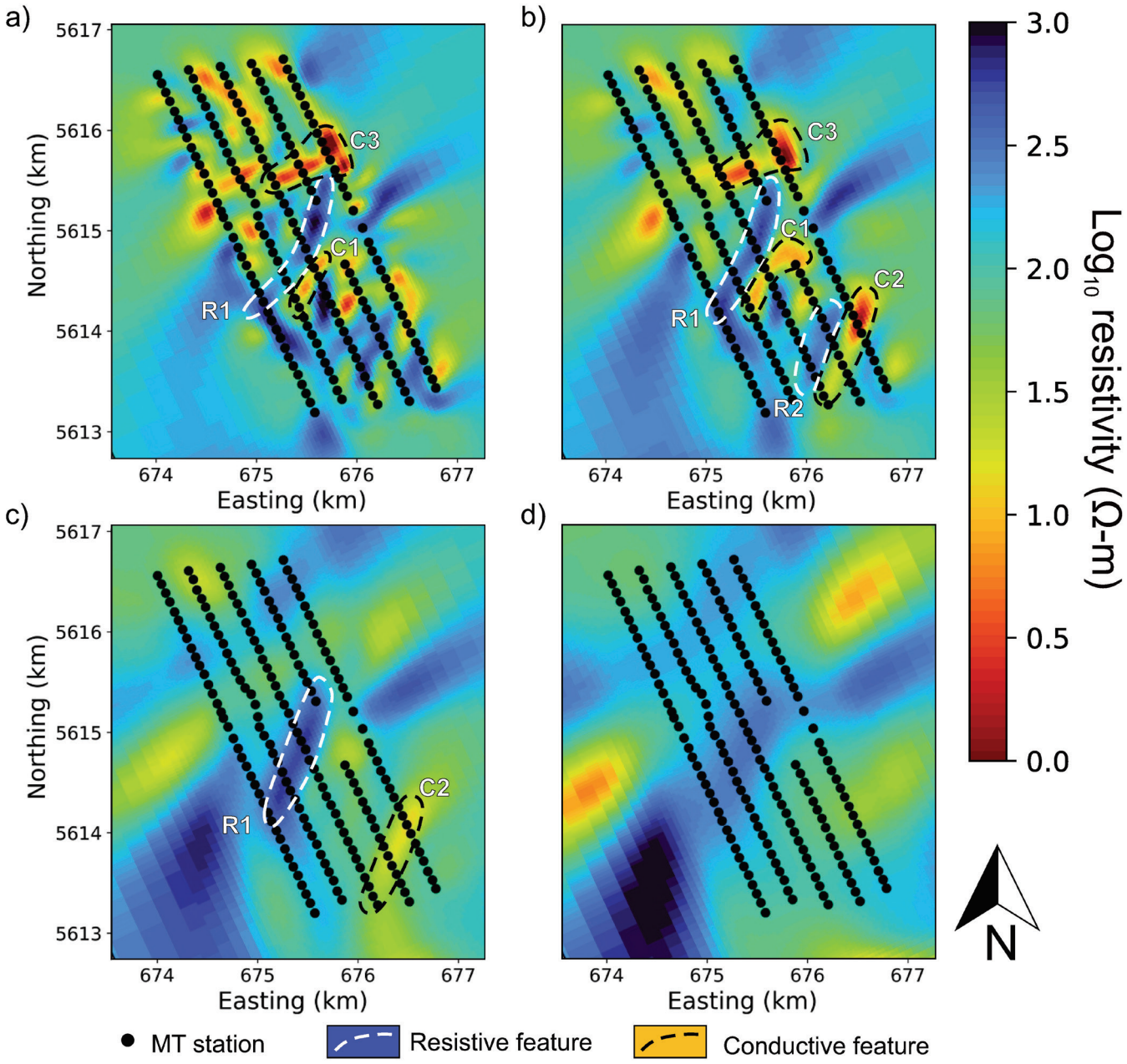

Figure 5. Plan view sections through the preferred model at various depths showing anomalous regions discussed in the text: **a)** 205 m, **b)** 316 m, **c)** 562 m, and **d)** 1000 m. The model and stations have been rotated back to geographic coordinates.

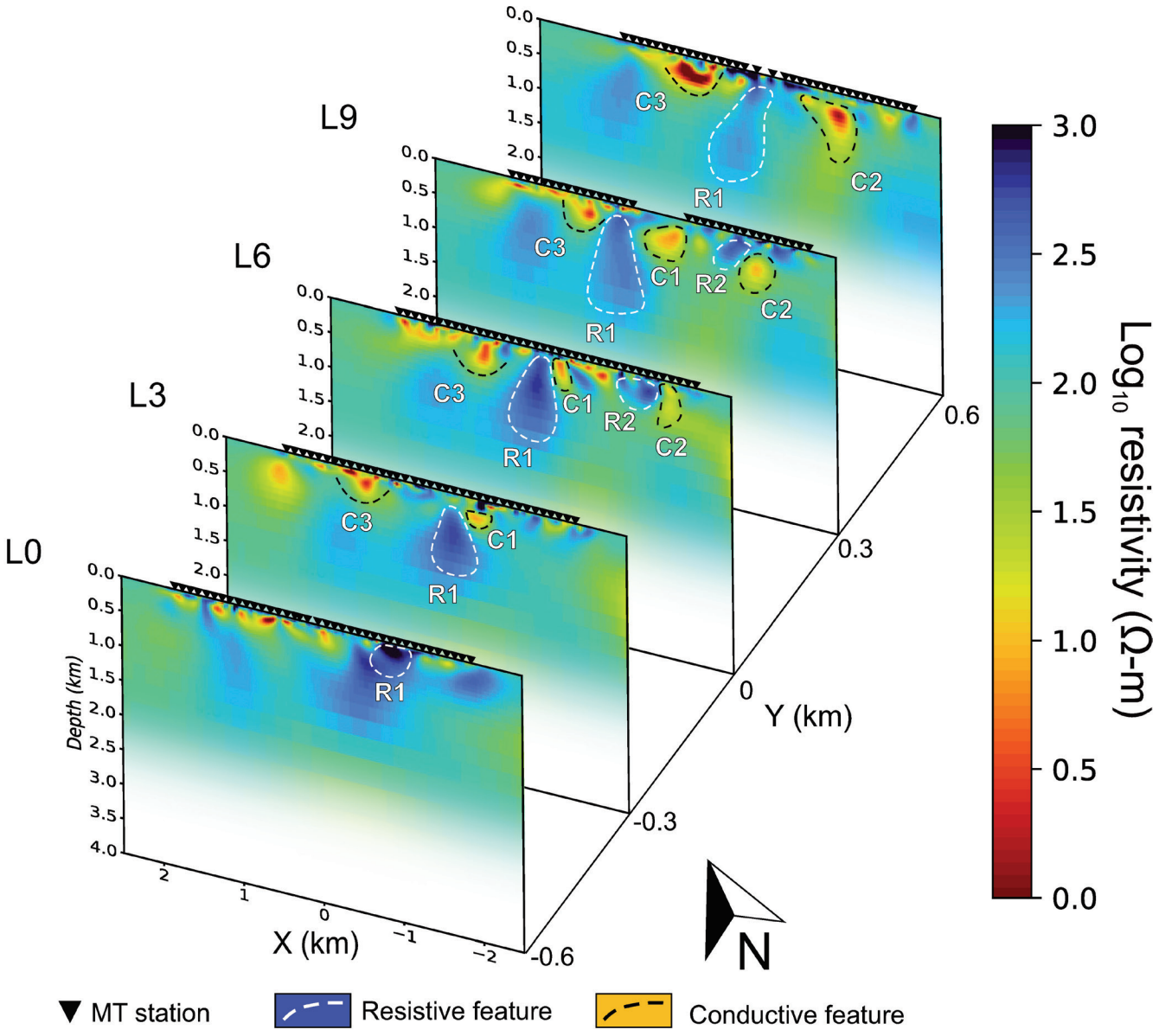

Figure 6. Depth slices through the focused model, coincident with the magnetotelluric (MT) lines, showing features discussed in the text.

resistive compared to the picrite unit; consequently, given the lack of evident relationships with primary lithological composition, hypogene mineralization, and alteration, we prefer an interpretation where secondary porosity, genetically associated with displacement along the previously mentioned southwest-northeast-trending fault zones, was favourable for generating resistivity contrasts. In addition, hydrothermal brecciation in combination with the fracture-controlled sulfide mineralization of the Pothook mineralization (in contrast to the disseminated sulfide mineralization of the New Afton) could provide an explanation for the more prominent conductor C2.

Patterns of alternating high- and low-resistivity linear features (e.g. C1/R1, C2/R2) have been identified as an artefact of isotropic inversions attempting to fit anisotropic data (e.g. Wannamaker, 2005; Miensopust and Jones, 2011). Although the possibility of anisotropy is impossible to fully dismiss without vertical magnetic field data, the phase of the data is generally well behaved at the relevant stations (e.g. smoothly varying and between 0–90°).

Contrary to the samples of the host rocks of the mineralization, the three samples of sandstone of the Kamloops Group in Figure 2a lend some support to interpreting the low resistivity of C3 as being due to primary porosity. The three samples plot on the low-resistivity high extreme of the

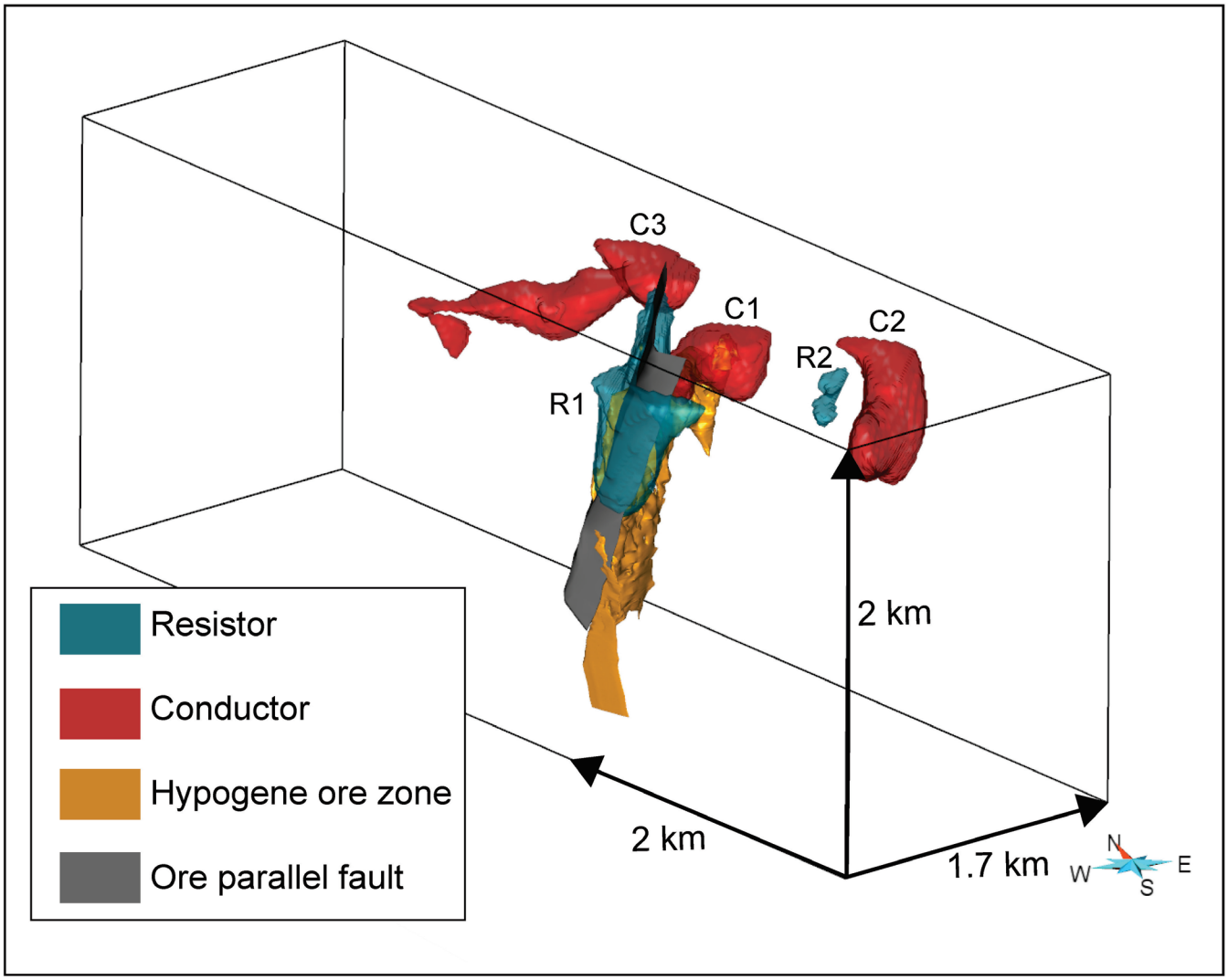

Figure 7. A 3-D view of resistive and conductive features in relation to models of the hypogene ore and northwest-southeast-striking fault zone discussed in the text. Resistive features were defined using a Log10 resistivity threshold of >2.5 (316 Ω-m). Conductive features were defined using a Log10 resistivity threshold of <1.5 (32 Ω-m).

scatterplot with more than 10% porosity. A notable increase in resistivity is seen at approximately 562 m deep, which may mark the base of the sediments. This interpretation is consistent with interpretation of 2-D MT inversions acquired in the Nechako Basin, where stratigraphically equivalent, shallowly dipping Eocene volcanic and sedimentary rocks are prominently marked by low resistivity in contrast with the underlying basement (Spratt and Craven, 2011). It is, however, worth noting that the location of C3 is coincident with power lines north of the open pit (and therefore with the stations with high noise and misfit), so the possibility that C3 is related to cultural noise rather than to geology cannot be ruled out. A feature test on C3 was carried out, whereby the conductive region was replaced with the original background resistivity (100 Ω-m). The resulting model response has an RMS misfit of 2.55, representing a 50% increase from the original inversion result. This suggests that, although the exact geometries and resistivity values are not resolvable due to the high degree of noise in the area, the data do require a conductive body in the vicinity of C3.

CONCLUSIONS

A high-density AMT survey was conducted over the New Afton Cu-Au porphyry deposit, British Columbia, Canada. Analysis of the MT data revealed generally low resistivities and 2-D geo-electric characteristics within a frequency band of 10 to 1000 Hz. At frequencies lower than 10 Hz, and therefore at greater depths, 3-D effects are evident. To image the structural controls on mineralization below the conductive cover, 3-D inversions were performed. Focused inversions in the area around the mineralized zone revealed low resistivities to the north, possibly related to a porous and

interconnected network of fluid within the Kamloops Group sedimentary rocks. Two high- and low-resistivity anomalies that are roughly coincident with the known economic mineralization in the area were imaged with a dominant southwest-northeast strike. Because the primary orientation of the lithological units is east-west and drill core resistivity is independent from the sampled lithological units, we determined that these anomalies are likely related to variations in secondary porosity genetically associated with the southwest-northeast-trending fault zones. In contrast to the poor association between the low resistivity feature at New Afton and its hypogene ore zone, the more prominent low resistivity feature at the Pothook deposit does coincide with its hypogene sulfide mineralization. This is explained by differences in the style of mineralization between the two deposits. The hypogene ore zone at New Afton consists of disseminated mineralization, whereas the Pothook mineralization is controlled by hydrothermal brecciation and tectonic fracturing, which both enhanced secondary porosity and the connectivity of sulfide mineralization in the volcanic and intrusive host rocks.

Due to the high density of MT stations and generally low resistivities of the survey area, it was not possible to model the entire data set with the available computational resources. In the future, a 3-D inversion of the entire data set may become feasible, which would allow high-resolution imaging of the New Afton deposit at greater depths and might provide additional control on its extent and geometry. It was determined that anisotropy is not likely to have had an impact on the isotropic inversion results, but it is also possible to investigate this further by performing 2-D anisotropic inversions. Future forward modelling and/or inversion studies would also benefit from inclusion of constraints derived from other geological or geophysical data sets.

ACKNOWLEDGMENTS

We gratefully acknowledge the support of New Gold Ltd., who provided access to their drillhole and MT data (collected by Quantec Geoscience Ltd.) and shared their expertise on the New Afton Cu-Au deposit. This manuscript benefited from reviews by Ademola Adetunji and Seyed Masoud Ansari.

REFERENCES

Bellefleur, G., Schetselaar, E., Wade, D., White, D., Enkin, R., and Schmitt, D. R., 2019. Vertical seismic profiling using distributed acoustic sensing with scatter-enhanced fibre-optic cable at the Cu–Au New Afton porphyry deposit, British Columbia, Canada; Geophysical Prospecting, v. 68, no. 1, p. 1–21. https://doi.org/10.1111/1365-2478.12828

Bergen, D., Krutzelmann, H., and Rennie, D.W., 2015. Technical report on the New Afton mine, British Columbia, Canada, NI 43-101 report; Roscoe Postle Associates Inc., Project #2400.

Booker, J.R., 2014. The magnetotelluric phase tensor: a critical review; Surveys in Geophysics, v. 35, no. 1, p. 7–40. https://doi.org/10.1007/s10712-013-9234-2

Caldwell, T.G., Bibby, H.M., and Brown, C., 2004. The magnetotelluric phase tensor; Geophysical Journal International, v. 158, no. 2, p. 457–469. https://doi.org/10.1111/j.1365-246X.2004.02281.x

Constable, S.C., Parker, R.L., and Constable, C.G., 1987. Occam's inversion: a practical algorithm for generating smooth models from electromagnetic sounding data; Geophysics, v. 52, no. 3, p. 289–300. https://doi.org/10.1190/1.1442303

de Groot-Hedlin, C. and Constable, S., 1990. Occam's inversion to generate smooth, two-dimensional models from magnetotelluric data; Geophysics, v. 55, no. 12, p. 1613–1624. https://doi.org/10.1190/1.1442813

Egbert, G.D. and Kelbert, A., 2012. Computational recipes for electromagnetic inverse problems; Geophysical Journal International, v. 189, no. 1, p. 51–267. https://doi.org/10.1111/j.1365-246X.2011.05347.x

Enkin, R.J., Cowan, D., Tigner J., Severide, A., Gilmour, D., Tkachyk, A., Kilduff, M., Vidal, B. and Baker, J., 2012. Physical property measurements at the GSC Paleomagnetism and Petrophysics Laboratory, including electric impedance spectrum methodology and analysis; Geological Survey of Canada, Open File 7227, 42 p. https://doi.org/10.4095/291564

Farquharson, C.G. and Craven, J.A., 2009. Three-dimensional inversion of magnetotelluric data for mineral exploration: An example from the McArthur River uranium deposit, Saskatchewan, Canada; Journal of Applied Geophysics, v. 68, no. 4, p. 450–458. https://doi.org/10.1016/j.jappgeo.2008.02.002

Heinson, G., Didana, Y., Soeffky, P., Thiel, S., and Wise, T., 2018. The crustal geophysical signature of a world-class magmatic mineral system; Scientific Reports, v. 8, 10608, p. 1–6. https://doi.org/10.1038/s41598-018-29016-2

Heinson, G.S., Direen, N.G., and Gill, R.M., 2006. Magnetotelluric evidence for a deep-crustal mineralizing system beneath the Olympic Dam iron oxide copper-gold deposit, southern Australia; Geology, v. 34, no. 7, p. 573–576. https://doi.org/10.1130/G22222.1

Jones, A.G., Evans, R.L., Muller, M.R., Hamilton, M.P., Miensopust, M.P., Garcia, X., Cole, P., Ngwisanyi, T., Hutchins, D., Fourie, C.J.S., Jelsma, H., Evans, S., Aravanis, T., Pettit, W., Webb, S., Wasborg, J., and The SAMTEX Team, 2009. Area selection for diamonds using magnetotellurics: examples from southern Africa; Lithos, Proceedings of the 9th International Kimberlite Conference, v. 112, suppl 1, p. 83–92. https://doi.org/10.1016/j.lithos.2009.06.011

Kelbert, A., Meqbel, N., Egbert, G.D., and Tandon, K., 2014. ModEM: a modular system for inversion of electromagnetic geophysical data; Computers and Geosciences, v. 66, p. 40–53. https://doi.org/10.1016/j.cageo.2014.01.010

Miensopust, M.P. and Jones, A.G., 2011. Artefacts of isotropic inversion applied to magnetotelluric data from an anisotropic Earth; Geophysical Journal International, v. 187, no. 2, p. 677–689. https://doi.org/10.1111/j.1365-246X.2011.05157.x

Miensopust, M.P., Queralt, P., Jones, A.G., and the 3D MT modellers, 2013. Magnetotelluric 3-D inversion—a review of two successful workshops on forward and inversion code testing and comparison; Geophysical Journal International, v. 193, no. 3, p. 1216–1238. https://doi.org/10.1093/gji/ggt066

Newman, G.A., 2014. A review of high-performance computational strategies for modeling and imaging of electromagnetic induction data; Surveys in Geophysics, v. 35, no. 1, p. 85–100. https://doi.org/10.1007/s10712-013-9260-0

Siripunvaraporn, W., Egbert, G., Lenbury, Y., and Uyeshima, M., 2005. Three-dimensional magnetotelluric inversion: data-space method; Physics of the Earth and Planetary Interiors, v. 150, p. 3–14. https://doi.org/10.1016/j.pepi.2004.08.023

Spratt, J. and Craven, J., 2011. Near-surface and crustal-scale images of the Nechako basin, British Columbia, Canada, from magnetotelluric investigations; Canadian Journal of Earth Sciences, v. 48, no. 6, p. 987–999. https://doi.org/10.1139/e10-098

Stanley, C. R., 1994. Geology of the Pothook alkalic copper-gold porphyry deposit, New Afton mining camp, British Columbia (92I/ 9 10); British Columbia Geological Fieldwork 1993, British Columbia Ministry of Energy, Mines and Petroleum Resources, Paper 1994-1, p. 275–284.

Stevens, K.M. and McNeice, G., 1998. On the detection of Ni-Cu Ore hosting structures in the Sudbury Igneous Complex using the magnetotelluric method; *in* SEG Technical Program Expanded Abstracts; Society of Exploration Geophysicists, p. 751–755. https://doi.org/10.1190/1.1820581

Türkoğlu, E., Unsworth, M., and Pana, D., 2009. Deep electrical structure of northern Alberta (Canada): implications for diamond exploration; Canadian Journal of Earth Sciences, v. 46, no. 2, p. 139–154. https://doi.org/10.1139/E09-009

Wannamaker, P. E., 2005. Anisotropy versus heterogeneity in continental solid earth electromagnetic studies: fundamental response characteristics and implications for physicochemical state; Surveys in Geophysics, v. 26, no. 6, p. 733–765. https://doi.org/10.1007/s10712-005-1832-1

Zhang, P., Chouteau, M., Mareschal, M., Kurtz, R., and Hubert, C., 1995. High-frequency magnetotelluric investigation of crustal structure in north-central Abitibi, Quebec, Canada; Geophysical Journal International, v. 120, no. 2, p. 406–418. https://doi.org/10.1111/j.1365-246X.1995.tb01828.x